THE ASTROPHYSICAL JOURNAL, 289:792–802, 1985 February 15

THE FRACTION OF HIGH VELOCITY DISPERSION H I IN THE GALAXY

SHRINIVAS R. KULKARNI AND MICHEL FICH[1]
Radio Astronomy Laboratory, University of California at Berkeley
Received 1984 June 28; accepted 1984 September 6

ABSTRACT

It has been recently suggested that a significant fraction of the neutral hydrogen clouds in our Galaxy have a cloud-cloud velocity dispersion of 35 km s^{-1} (Radhakrishnan and Srinivasan). This was found from an analysis of an H I absorption profile toward the galactic center and was further supported by comparisons of H I absorption profiles and radio recombination line profiles toward H II regions (Anantharamaiah, Radhakrishnan, and Shaver; Shaver *et al.*).

Using H I emission data, we find that, indeed, a detectable amount of higher than normal velocity-dispersion H I exists. However, the fraction of H I in these clouds is about an order of magnitude less than that suggested by Radhakrishnan and Srinivasan. This "fast" H I constitutes less than 5% of the volume density of the H I in the galactic plane and has a higher scale height than the normal velocity-dispersion H I clouds. It probably constitutes $\leq 20\%$ of the total mass of galactic H I but contains most of the kinetic energy of the ISM. Despite this, the rate of energy required to keep this fast H I layer stirred up is smaller by an order of magnitude than the equivalent rate for normal H I clouds.

We find that the statistics of H I clouds deduced from H I absorption/H II region recombination data depend very critically on a host of systematic errors. After accounting for all these effects, we find that the conclusions of Anantharamaih, Radhakrishnan, and Shaver and Shaver *et al.* are considerably weakened.

Subject headings: galaxies: Milky Way — interstellar: matter — radio sources: 21 cm radiation

I. INTRODUCTION

Conventionally, most of the mass of the interstellar medium (excluding the molecular ring) is thought to be in cold, neutral hydrogen clouds which have a cloud-cloud velocity dispersion of 5–7 km s^{-1} and also in an intercloud medium of warmer H I, which has a dispersion of 7–9 km s^{-1} (Lizst 1983; Burton 1976). However, recent reinterpretation of some observations has led to a suggestion that there may also be a considerable amount of neutral hydrogen with a significantly larger velocity dispersion.

Based on an analysis of an H I absorption spectrum toward the galactic center, Radhakrishnan and Srinivasan (1980; hereafter RS) postulate and discuss the existence of a new class of neutral hydrogen clouds with a cloud-cloud dispersion of 35 km s^{-1}. The basis for this assertion was a reanalysis of a Parkes H I absorption spectrum toward the galactic center by Radhakrishnan and Sarma (1980) which showed a deep, narrow feature and a shallow, broad feature both centered at 0 km s^{-1}. In this direction ($l = 0°$, $b = 0°$) the structure in the spectrum of H I is independent of galactic rotation and is thus an ideal line of sight for the determination of the velocity dispersion of H I. RS interpreted the narrow feature to arise from the normal dispersion cold clouds and the broad feature to arise from larger dispersion clouds. Comparison of a Bonn H I emission spectrum with the absorption data led to the following properties for the clouds: $N_H \leq 10^{20}$ cm^{-2}, $N_H/kpc \approx 2 \times 10^{21}$ cm^{-2} kpc^{-1}, $T_s \approx 300$ K, and an rms cloud-cloud velocity dispersion of 35 km s^{-1}.

The implications of this result, if true, are enormous. The kinetic energy in the new class of clouds, appropriately called "shocked clouds," is ~ 100 times that in the cold normal dispersion clouds. The average density of these clouds *in the galactic plane* is twice that of the cold clouds. Also, if these clouds are in gravitational equilibrium with the stellar disk, and thus have a large scale height in the z direction, then they may contain as much as 80% of the H I in the Galaxy.

There are few other observations relevant to the RS model. A comparison of the extreme velocity of H I absorption profiles toward H II regions with radio recombination emission profiles has led Anantharamaiah, Radhakrishnan, and Shaver (1984; hereafter A) and Shaver *et al.* (1982; hereafter S) to support the conclusions of RS.

On the other hand, Schwartz, Ekers, and Goss (1982) analyzed an H I absorption spectrum toward the galactic center, which was obtained with the Westerbork Radio Synthesis Telescope, and placed an upper limit on the number density of shocked clouds. This upper limit is one-third of that proposed by RS. Even with this limit,tthe total mass of the shocked clouds could be as high as 3 times the total mass of the cold clouds.

In this paper we intend to estimate the fraction of clouds which make up this high velocity dispersion H I. In § II we compare observed H I *emission* profiles to synthetic profiles to obtain a firm upper limit to the fraction of high dispersion H I for the inner Galaxy, at the solar circle and beyond the solar circle. In § III we discuss the difficulties in using H II regions for this kind of analysis and suggest alternative explanation for the observations described by S and A. In § IV we examine the effect of the fast H I on the energy balance within the interstellar medium. We summarize our results in § V.

II. CONSTRAINTS ON FAST CLOUD POPULATION FROM H I EMISSION DATA

The principal difficulty in using H I absorption data for estimation of H I cloud statistics is the necessary bias against

[1] Present address: Astronomy Department, University of Washington, Seattle, WA.

warmer H I. The optical depth in H I is proportional to N_H/T, where N_H is the column density and T is the temperature. Since the high velocity dispersion H I ("fast H I") is probably the result of shocks, it could be warmer and, therefore, more optically thin than the colder, "slow" H I. On the other hand, H I emission is proportional to N_H in the optically thin limit, and hence its use does not result in any bias against warm clouds.

For this reason we construct synthetic emission profiles based on the parameters suggested for both the "slow" and the "fast" clouds. These synthetic profiles are then compared to the observed profiles in various directions. Since H I is found in emission in almost every direction in the sky and over a wide range of radial velocities, the data must be chosen carefully. We only chose data in the "forbidden velocity" ranges, i.e., those velocity ranges over which no gas should exist, assuming strict circular rotation and zero velocity dispersion. The amount of gas at various forbidden velocities is then a measure of the velocity dispersion.

We construct synthetic profiles of H I at these forbidden velocities using three parameters: σ_s and σ_f, which are the velocity dispersions of the slow (cold) and fast (shocked) H I, and N_s/N_f, the ratio of the column densities of the slow and fast clouds. We then fit the observed profile over the forbidden velocities by varying the total column density (i.e., $N_s + N_f$) and the velocity zeropoint. The value of the mean-squared deviation between the observed and synthetic profiles is then a measure of the "goodness" of the fit for the particular input parameters. We have made no attempt to explain the structure in the observed spectrum at allowed velocities since that arises from galactic rotation and the galactic distribution of normal H I clouds—both of which are fairly well understood.

a) H I *in the Inner Galaxy*

Here we consider H I beyond the subcentral velocity, which is the extreme velocity expected due to galactic rotation along a line of sight through the "inner Galaxy" (i.e., inside the solar circle). In Figure 1 we have plotted the H I profile at $l = 30°$, $b = 0°$ taken from the Weaver and Williams (1973) H I survey. This longitude was chosen because the radial distribution of supernova remnants and other young objects in our Galaxy shows a peak near $R = 5$ kpc, and this line of sight is tangential to a circle of that radius. Thus, if shocked clouds are the products of supernova shocks, one would expect to see the largest number of such clouds at the subcentral velocity appropriate to this longitude.

Plotted with a dashed line is a "good fit" (i.e., low rms deviation between the model and the observations) two-component model. That this is not a unique fit should be evident from Figure 2 in which another equally good fit is shown. Taken together, these figures show two trends which are evident in all the good fits: (1) σ_s is ~ 7.7 km s^{-1} and (2) larger values of σ_f require larger values of the ratio N_s/N_f; basically, the product of the height and the width of the high dispersion component is constant. Even if the fast gas has a velocity dispersion as low as 14 km s^{-1}, it cannot have a fractional volume density greater than 12% in the galactic plane. If this gas has a velocity dispersion as high as 30 km s^{-1}, the fractional volume density in the galactic plane cannot be more than 4%. An inspection of the H I emission spectra at other inner galaxy longitudes shows similar behavior.

b) H I *in the Solar Neighborhood*

In this subsection we analyze the H I seen in emission in the solar neighborhood and show that most of the H I either has a velocity dispersion of 6 km s^{-1} or ~ 14 km s^{-1}. We identify the 6 km s^{-1} dispersion gas with the diffuse H I clouds and the 14 km s^{-1} with the warm, intercloud gas.

To examine only nearby H I it is necessary to look out of the galactic plane. Accordingly, we have averaged all the normalized profiles (i.e., after multiplying the profiles by $|\sin b|$) of the

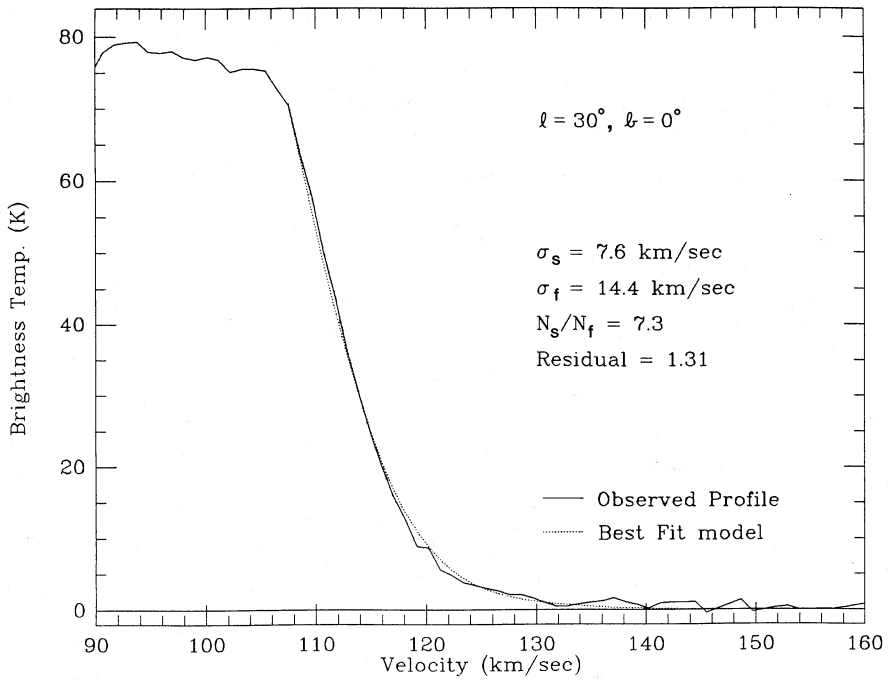

FIG. 1.—Comparison of the observed profile (*thick line*) toward $l = 30°$, $b = 0°$ with a two-component Gaussian model (*dashed line*). The Gaussian parameters are shown in the right half of the figure. The fit was restricted to only velocities beyond 107 km s^{-1}, the subcentral point velocity. The tail is represented by the sum of two error functions corresponding to the two components. Such a simplified model is adequate to describe the long tail produced by the fast H I.

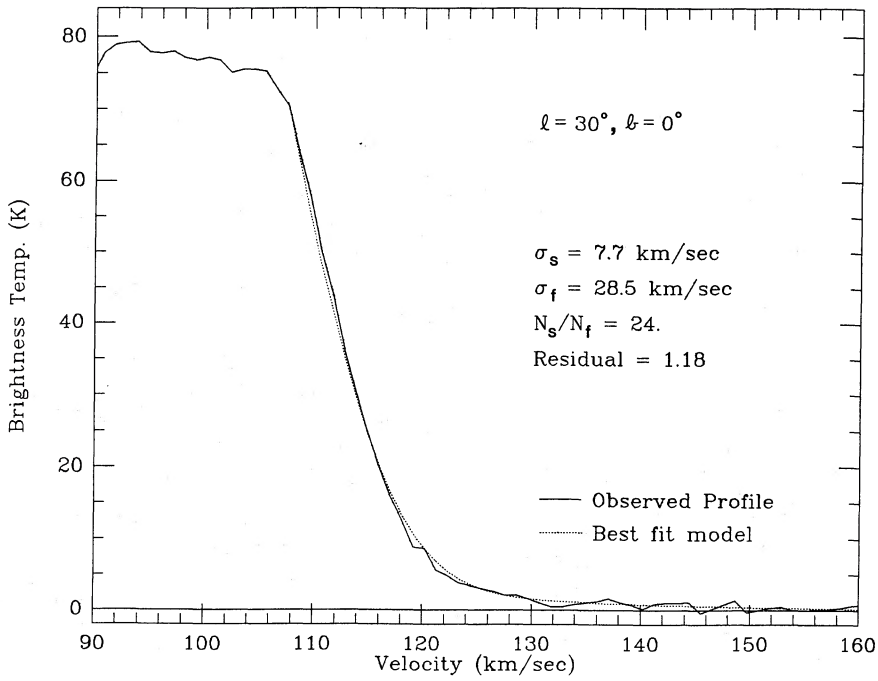

FIG. 2.—Comparison of the observed profile (*thick line*) toward $l = 30°$, $b = 0°$ with a two-component gaussian model (*dashed line*). As in Fig. 1, the fit was restricted to velocities greater than 107 km s^{-1}. Note that this fit not only has a somewhat smaller residual but also accounts for the high-velocity H I quite satisfactorily.

AT&T Bell Laboratories (BL) H I survey (Stark *et al.* 1984; data kindly provided by A. Stark and C. Heiles) for $90° > b > 75°$, $0° < l < 360°$ and $-90° < b < -70°$, $0° < l < 360°$. These are displayed in Figures 3 and 4, respectively. The longitude coverage is complete for the north galactic pole (NGP) region but is somewhat incomplete for the south galactic pole (SGP) region because of the southern declination limit of the BL H I survey. We have checked the Argentine H I survey (Coulomb, Popper, and Heiles 1974) for the longitude range that is missing in the BL H I survey and find that our average shown in Figure 4 is unbiased by the incomplete coverage. The BL H I survey is eminently suitable for this exercise because, unlike other radio telescopes, the BL horn antenna receives very little scattered radiation. Consequently, we can place trust in the reality of the faint H I emission that can be seen in Figures 3 and 4.

From Figure 3 we see that in the NGP region a substantial amount of H I is falling toward the galactic plane. This is a well-known result (e.g., Weaver 1974). The spectrum peaks roughly around -2 km s^{-1} and the H I distribution for $v > -2$ km s^{-1} appears quiescent in comparison. We take the view that this quiescent H I is more representative of the typical H I and that most of the H I for $v < -2$ km s^{-1} is "abnormal" in the sense that it is probably peculiar to our local neighborhood and not characteristic of H I on a galactic scale. Arguments in favor of this viewpoint are (*a*) the single-dish H I emission spectra of face-on spiral galaxies do not show infall at such high levels (Lewis 1983), and, more importantly, (*b*) the H I emission toward the SGP region (Fig. 4) does not show infall at such a high level. In order to obtain the velocity dispersion of the local "normal" H I we have only used the H I in Figure 3 which is at $v \geq -2$ km s^{-1}. In Figure 5 this part of the spectrum has been decomposed into two Gaussians. We have carried out a similar exercise for the SGP region using the H I with $v \geq -6$ km s^{-1}.

From Figure 5 it should be clear that the RS model overestimates the amount of fast H I by a factor of ~ 5. In contrast, our two-component model underestimates the amount of fast H I. Because of the nonuniqueness of the Gaussian decomposition we have not attempted to add another high velocity dispersion component to account for the observed profile in Figure 5 at all velocities. Instead, in Table 1 we compare the fraction of observed H I unaccounted for by our model with the model prediction. Assuming that fast H I is characterized by a Gaussian velocity distribution with a σ of 35 km s^{-1} and noting that $f(|v| > 30$ km s$^{-1})$ is 6.3%, we find that that the fraction of fast H I is $\sim 20\%$. Note that this fraction refers to *mass fraction.*

Now we discuss in detail the two-component model of Figure 5, the parameters of which are given in Table 2. For each Gaussian component, the height and the width (FWHM) are given in columns (2) and (3); the corresponding values of the velocity dispersion and column density are shown in columns (4) and (5), respectively. Column (6) shows the total observed column density. Column (7) represents the column density not accounted for by our two-component model and an indicator of the amount of H I that is not symmetrically distributed about the adopted mean velocity. The error in each of the

TABLE 1

COMPARISON OF DATA AND MODEL

V (km s^{-1})	$f(\|v\| > V)$ (observed)	$f(\|v\| > V)$ (two-component model)
22	10.0%	7.6%
30	6.3%	2.0%
50	3.8%	0.02%
100	1.0%	0.00%

NOTES.—$f(|v| > V)$ refers to the column density fraction of H I with velocity $|v| > V$. The profiles shown in Fig. 5 were used to compute this table.

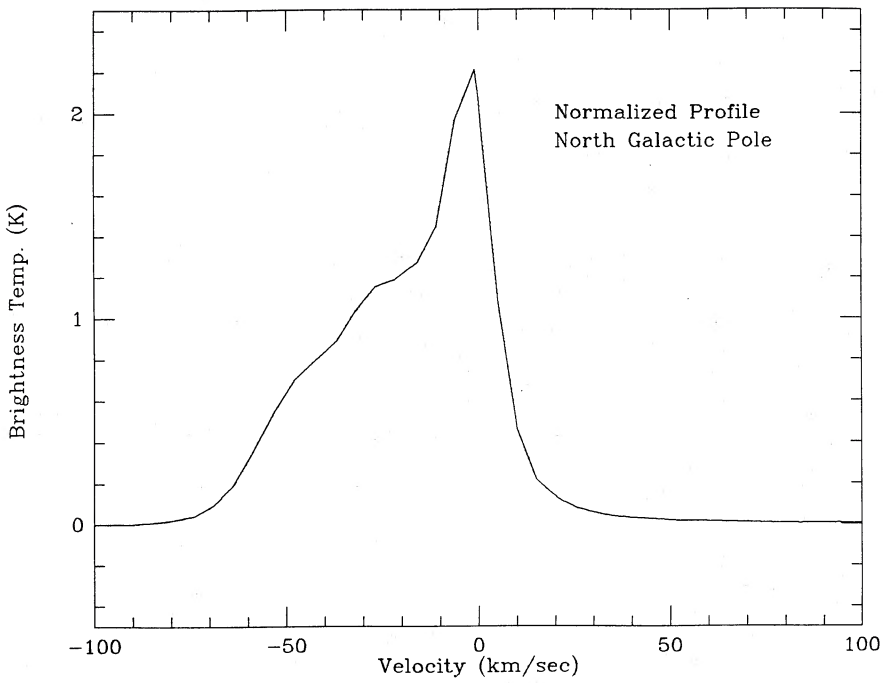

FIG. 3.—The mean profile toward the north galactic pole (NGP). All profiles with $90° > b > 75°$ and $0° < l < 360°$ of the Bell Telephone Laboratories H I survey after multiplication by $|\sin b|$ have been averaged to form this mean profile. Note the highly asymmetric profile. More than half of all H I is falling toward the galactic plane.

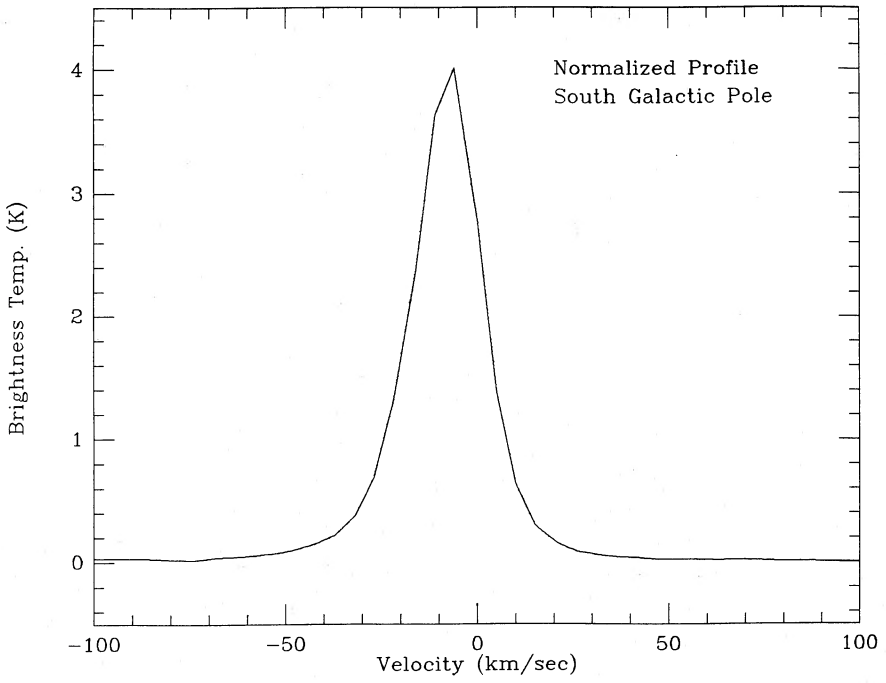

FIG. 4.—The mean profile toward the south galactic pole (SGP). The mean profile was formed the same way as in Fig. 3, except that the latitude range is $-90° < b < -70°$. The profile appears to be centered ~ -6 km s^{-1}. Note that there is more H I toward the south pole, and furthermore the infall is considerably less than that at the NGP (Fig. 3).

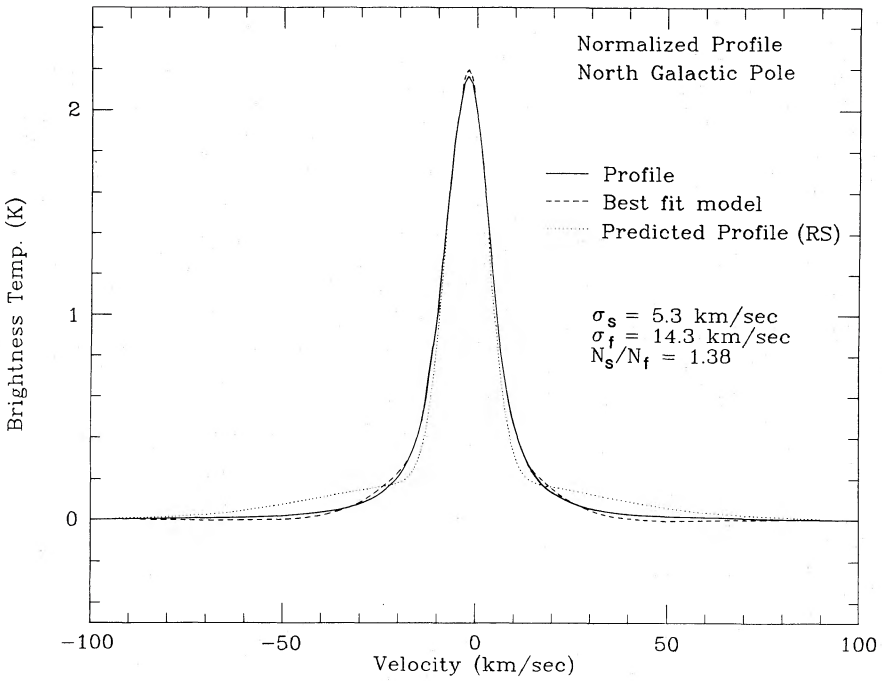

FIG. 5.—Model NGP profile used for Gaussian analysis. The model profile was obtained by reflecting the profile shown in Fig. 4. around $v = -2$ km s^{-1}. The Gaussian two-component fit was restricted to the NGP profile for $v > -2$ km s^{-1} in order not to be affected by the infall. Also shown are the predictions of the RS model and the best fit two-component Gaussian model. Note that the RS model overestimates the amount of high dispersion H I by a factor of 5, whereas our best fit model somewhat underestimates this H I.

quantities shown in Table 2 is ~25% and mainly arises from the fact that the Gaussian parameters do depend slightly upon the velocity assumed for the cutoff (i.e., the velocity of the peak).

We identify component 1 with the clouds that appear in 21 cm absorption and component 2 with a part of the "Not Strongly Absorbing" gas (NSA) of Dickey, Salpeter, and Terzian (1979). We associate the narrow Gaussian component with the cold clouds that are seen in 21 cm absorption because the dispersion of this component is approximately that of the 21 cm absorption clouds. The NSA as defined by Dickey, Salpeter, and Terzian (1979) is composed of three distinct types of H I: (*a*) the wings of the absorption lines, (*b*) H I with low brightness temperature which for any reasonable spin temperature would have optical depth lower than the sensitivity of the Arecibo survey, and (*c*) the truly warm ($T \approx 8000$ K) intercloud H I. A reasonable decomposition of the NSA would then attribute most of the low velocity ($|v| < 10$ km s^{-1}) with (*a*) and (*b*). Hence, we feel quite confident in associating the wide Gaussian component with the warm, intercloud medium H I. We conclude by noting that both in the NGP and the SGP areas ~40% ± 10% of the H I is warm H I with a dispersion exceeding the dispersion arising from its thermal temperature by ~50%.

It is well known that we are living in a local hole presumably caused by a supernova (e.g., Paresce 1984). Thus, the paucity of the fast clouds in our local neighborhood in comparison to the predictions of the RS model cannot be attributed to the absence of an energetic source.

Some other interesting results are that in the NGP area ~50% (see col. [7] of Table 2) of the H I is "abnormal" H I which is falling toward the plane at an average modest velocity of few tens of kilometers per second. In the SGP region ~25% of H I is "abnormal" H I and, in addition, is also flowing toward the galactic plane but with a somewhat lower velocity.

TABLE 2

RESULTS FROM TWO-COMPONENT MODEL

Component (1)	Height (K) (2)	FWHM (km s^{-1}) (3)	σ (km s^{-1}) (4)	N_H (10^{18} cm^{-2}) (5)	N_H (observed) (10^{18} cm^{-2}) (6)	N_H (unaccounted) (10^{18} cm^{-2}) (7)
North Galactic Pole						
1	1.73	12.4	5.3	39	154	87
2	0.46	33.7	14.3	28	...	...
South Galactic Pole						
1	3.02	16.4	7.0	90	184	54
2	0.74	36.9	15.7	50	...	...

Not surprisingly, this abnormal H I has a higher spin temperature since this gas mainly appears as NSA gas of Dickey, Salpeter, and Terzian (1979).

c) H I *in the Galactic Anticenter*

All nonzero velocities toward the galactic anticenter are "forbidden." In Figure 6 we have plotted an H I profile at $l = 180°$, $b = 0°$ taken from the Weaver and Williams (1973) survey. Notice that the observed profile in Figure 6 is not symmetrical about 0 km s^{-1} and, furthermore, appears to be made of at least three components centered at +8, 0, and −8 km s^{-1}. These correspond to well-identified large-scale features. Because of such large-scale streaming motions in this region, we have not tried to do any model fitting as in §§ II*a* and II*b*. Instead we have displayed in dashed lines in Figures 6 and 7 a two-component Gaussian model with $\sigma_s = 8.7$ km s^{-1}, $\sigma_f = 35$ km s^{-1} and $N_s/N_f = 4$. Figure 7 is simply a magnification of Figure 6 and is shown to facilitate a detailed comparison between the model and the observed profile. The model appears to give a reasonable fit for the negative-velocity tail but clearly overestimates the positive-velocity tail H I. The gas in the negative velocity tail arises mainly from discrete, well-identified intermediate and high velocity complexes and streams in the anticenter and has nothing to do with fast clouds (e.g., Kulkarni 1983 for a discussion of anamolous H I in this region and for further references). Thus, in the outer galaxy at $b = 0°$, the fractional *volume density* of fast H I ($|v| > 30$ km s^{-1}) is $<(N_s/N_f)(\sigma_f/\sigma_s) = 10\%$.

III. STATISTICS OF H I CLOUDS FROM H II REGION DATA

Both A and S use the statistics of the difference between the velocity of the H II region as measured from the radio recombination line ($V_{\rm H\,II}$) and the extreme velocity of the H I absorption features ($V_{\rm H\,I}$) to determine the random motions of H I. The underlying idea in both these papers is that the distribution of Δv(H I, H II) *solely* reflects the random motions of the H I clouds and hence can be used to find the number density and the velocity dispersion of the H I clouds. Here Δv(H I, H II) is the difference between $V_{\rm H\,I}$ and $V_{\rm H\,II}$, and the sign convention is so chosen that the sign of Δv is positive when the distance indicated by the H I absorption feature is greater than that implied by the H II region velocity. Unfortunately, both $V_{\rm H\,I}$ and $V_{\rm H\,II}$ are affected by systematic and random motions. That systematic motions can and do occur should be clear from the various examples discussed in § III*a*; indeed, such motions are expected on theoretical grounds. The biases in Δv(H I, H II) introduced by the systematic motions are discussed in § III*a* and that of random motions in § III*b*. In § III*c*, we conclude that, owing to these biases in Δv(H I, H II), the number density and the velocity dispersion of H I clouds inferred from the statistics of Δv(H I, H II) are unreliable.

a) *Systematic Motions*

There are two categories of systematic effects: (*a*) peculiar motions (i.e., motions in addition to the usual circular rotation) in the H II gas or in the H I associated with the H II region, or both; and (*b*) large-scale, noncircular motion of the H II region as a whole or of the intervening H I clouds, or both. The latter kind is well known to occur over large sections of the Galaxy (e.g., Burton 1976). These streaming motions have amplitudes of ~10 km s^{-1} for H I clouds and hence definitely introduce nonnegligible systematic biases in the statistics of Δv(H I, H II). However, because of the difficulty of estimating the magnitude of streaming motions along the lines of sight to the various H II regions of A and S, we confine the discussion here to the systematic effects arising from motions within or near the H II

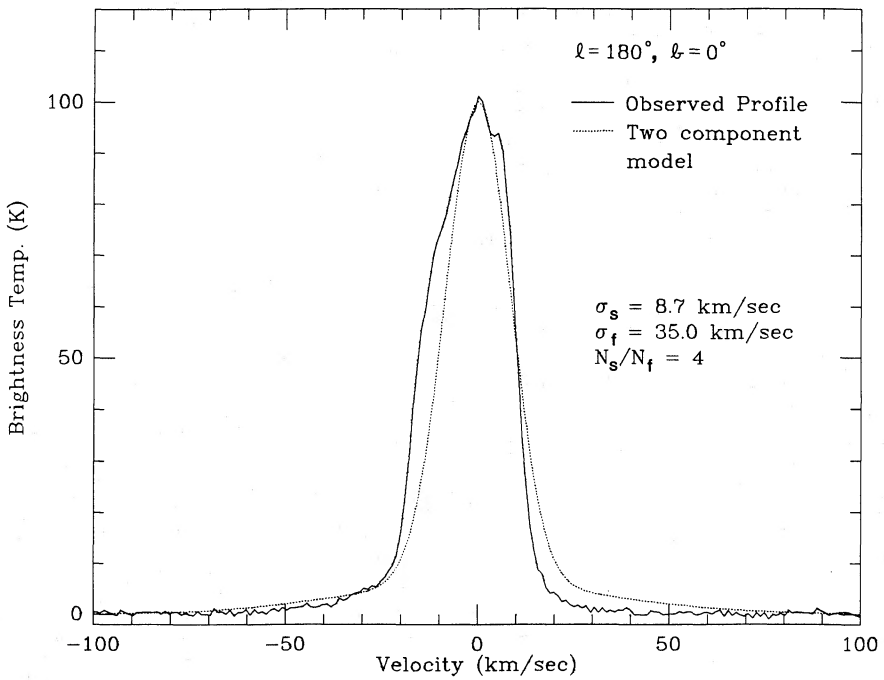

FIG. 6.—Comparison of the observed profile (*thick line*) toward $l = 180°$, $b = 0°$ with a two-component Gaussian model (*dashed lines*). A two-component fit was not attempted because of the large-scale streaming motions in this region. The Gaussian parameters for high dispersion H I are the ones suggested by RS. Note again, especially at large positive velocities, the RS model overestimates the amount of H I. The seemingly better fit for large, negative |velocities| is mainly due to an excess of intermediate velocity features that abound in the anticenter region (e.g., Kulkarni 1983).

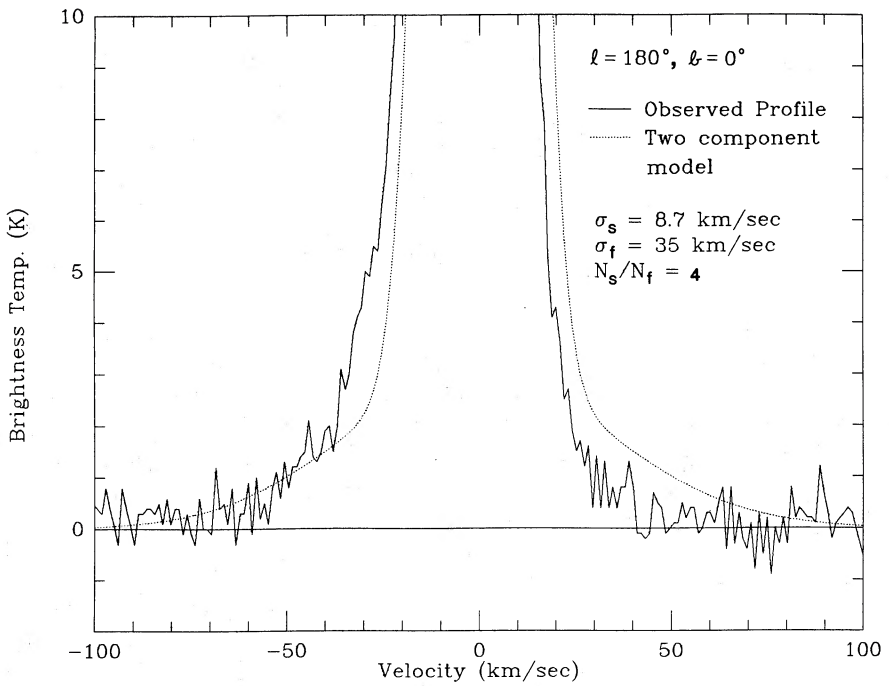

FIG. 7.—This is a magnification of Fig. 6 and is shown to facilitate a comparison between the model and the observed profile of the H I in the positive- and negative-velocity tail.

regions. Thus, we are underestimating the extent to which Δv(H I, H II) is affected by systematic motions. After the completion of our work, we became aware of a preprint by Bash and Leisawitz (1984) in which essentially the large Δv(H I, H II) H II regions are attributed to such motions; the estimates for the noncircular motions are estimated by the use of the ballistic theory for molecular clouds (Bash 1983).

A and S correctly argue that systematic motions lead to quadrant-dependent (i.e., galactic longitude) effects. To see such effects requires substantial amounts of data in at least two quadrants. However, most of the data of A and S come from the fourth quadrant, and, in particular, all the large Δv(H I, H II) regions other than M8 lie in the fourth quadrant. In addition, the signature (i.e., bias in Δv) of a given type of systematic motion could be masked by other types of systematic motions which bias Δv in an opposite fashion. For example, the outflow of the ionized gas relative to the neutral gas biases Δv(H I, H II) in a way that is opposite to the bias arising from an expanding H I shell—resulting in a smaller variation in Δv than from either motion alone and at the same time increasing the uncertainty in the inferred H I cloud-cloud velocity dispersion.

Now we consider the systematic motions that occur in or near the H II regions.

i) *Outflow of the Ionized Gas*

One expects to find large velocity motions in the ionized gas of some H II regions. A better representative of the "true" galactic velocity of the H II region is the velocity of the 3 mm CO line (V_{CO}) which arises in the much more massive parental molecular cloud. Figure 8 shows a histogram of Δv(CO, H II) for optical H II regions (Fich, Treffers, and Blitz 1982). There are two facts worth noting in Figure 8: (1) $\langle \Delta v(\mathrm{CO}, \mathrm{H\ II}) \rangle = 1.4\ \mathrm{km\ s^{-1}} \pm 0.4\ \mathrm{km\ s^{-1}}$, and (2) $\sigma[\Delta v(\mathrm{CO}, \mathrm{H\ II})] = 4.6\ \mathrm{km\ s^{-1}}$ *after correcting* for the measurement uncertainties in $V_{CO}[\sigma(V_{CO}) \approx 1\ \mathrm{km\ s^{-1}}]$ and $V_{H\,II}[\sigma(V_{H\,II}) \approx 3\ \mathrm{km\ s^{-1}}]$. These together imply that, on average, there is a slow outflow of ionized gas in H II regions and, furthermore, the velocity of an H II region, as a whole, could differ from the "true" galactic velocity by typically $\sigma[\Delta v(\mathrm{CO}, \mathrm{H\ II})]$. We utilize this constraint in § III*b*.

As argued in the preceding paragraph, V_{CO} is preferable to $V_{H\,II}$. With this in mind, we collected all the available V_{CO} data from the catalogs of Gillespie *et al.* (1977) and Blitz, Fich, and Stark (1983) and obtained Δv(H I, CO) for 23 of the 38 H II

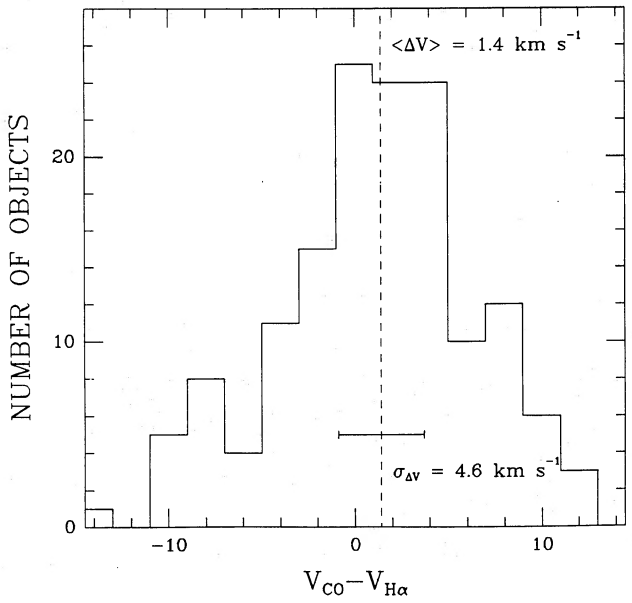

FIG. 8.—Difference between the CO and hydrogen-recombination line velocities in 155 optical H II regions (taken from Fich *et al.* 1980).

regions that were considered by A and S. Not surprisingly, for most of the objects Δv(H I, CO) remains close to the values of Δv(H I, H II). The major exceptions are (*a*) RCW 49, for which Δv(H I, H II) = 4.7 km s^{-1} and Δv(H I, CO) = -12.0 km s^{-1}; (*b*) RCW 117, for which Δv(H I, H II) = 10.7 km s^{-1} and Δv(H I, CO) = 15.5 km s^{-1}; and (*c*) M8, for which Δv(H I, H II) = 12.4 km s^{-1} and Δv(H I, CO) = 3.4 km s^{-1}. Thus, in RCW 49 and M8 there are clearly large differences between the velocity of the ionized gas and the center-of-mass velocity of the associated molecular cloud, indicating ionized gas outflows. Thus, M8, which was the only object in the first quadrant of the Galaxy with a large positive Δv in the data of A and S, is certainly an example of an object where systematic effects dominate, and the observed Δv(H I, H II) is not due to intervening high velocity dispersion H I clouds.

Of the 38 H II regions considered by A and S, 11 are in the first quadrant, one is in the second, five are in the third, and 23 are in the fourth. The objects with large Δv(H I, CO), a total of five, are all in the fourth quadrant. Considering that there are about half as many H II regions in the first quadrant as in the fourth, we expect to find two to three large Δv H II regions in the first quadrant and instead find none. This quadrant-dependent result clearly indicates that additional systematic effects are still present.

In passing, we would like to point out that four of the 23 H II regions (RCW 122, RCW 117, G351.7$-$1.2, and G333.6$-$0.2) are certainly outstanding because even their Δv(CO, H I) > 10 km s^{-1}. Thus, the discrepancy between the H II region velocity and the H I absorption cannot be attributed to outflow. At the present time, we offer no definitive explanation for these large Δv(CO, H I) H II regions except to remark that if these H II regions are similar to the ones discussed in § III*a*(ii) below, then the large Δv(CO, H I) imply expanding H I shells in these H II regions.

ii) *Expanding* H I *Shells around the* H I *Regions*

Theoretically one expects to see expanding H I shells as a result of ionization fronts around the H II regions or H I shells formed by dissociation of molecular hydrogen that is associated with the parental giant molecular cloud (e.g., Van Buren 1983). Several such examples can be found despite the paucity of the number of H I maps of galactic H II regions. Roger and Pedlar (1981) find an expanding, cold, dense H I shell ($6 < V_{sh} < 19$ km s^{-1}) in NGC 281, and Read (1980) reports an H I shell with $V_{sh} \approx 10$ km s^{-1} in the H II region NGC 7358; here V_{sh} is the shell expansion speed. Fich and Van Buren (1984) have recently mapped six H II regions in the second quadrant using the VLA. In four of them they find high optical depth ($\tau \approx 1$) H I absorption features with velocities typically more negative than the velocity of the H II region by $\sim$20 km s^{-1}. Higher resolution maps may clarify whether these H I absorption features are expanding shells around the H II region such as in NGC 281 or arise in high dispersion H I clouds along the line of sight to the H II region. However, the observed high optical depths rule out the fast, *warm* clouds envisaged by RS.

b) Random Motions

In the previous subsection we argued that V_{CO} is a better indicator of the "true" circular motion of the H II region than $V_{H\,II}$. This and the observed dispersion in the quantity Δv(CO, H II) (see § III*a* and Fig. 8) mean that even if the slow, intervening H I clouds had zero dispersion, the observed dispersion in Δv(H I, H II) should be 4.6 km s^{-1}. In the general case where the H I clouds have a dispersion σ, the dispersion in Δv should be $(4.6^2 + \sigma^2)^{1/2}$. Note that this is the *minimum* expected dispersion since it does not include contributions discussed in § III*a*. The σ for the cold clouds is well known, and the best determination is that by Schwarz, Ekers, and Goss (1982), who determine σ to be $\sim$5.3 km s^{-1} from a Westerbork synthesis absorption spectrum toward the galactic center. Thus, the dispersion for the cold clouds deduced from the statistics of Δv should be at least $(5.3^2 + 4.6^2)^{1/2} = 7.0$ km s^{-1}. In contrast to this, S and A deduce dispersions of 4.8 and 4.1 km s^{-1}, respectively, which is less than the minimum expected value for the observed dispersion of the cold clouds. Restating this contradiction in another way, the dispersion for the cold clouds, after accounting for the flow of the ionized gas in the H II regions relative to the parental cloud, is about 0 and 1 km s^{-1}, respectively.

c) Problems of the Statistics of Δv(H I, H II)

The use of the distribution of Δv(H I, H II) for determining the cloud number density and velocity dispersion is, in principle, correct. However, systematic effects, such as the ones outlined in § III*b*, do contaminate the statistics and make the ensuing results uncertain. For example, the σ for slow, cold H I clouds, corrected for the motion between the parental molecular cloud and the ionized gas, is $\sim$0 and $\sim$1 km s^{-1}. This inadmissably low value probably arises because a two-component fit for Δv(H I, H II) was used by both A and S. In general, when two-component fits are used for data whose underlying distribution has only one component, then the two model dispersions bracket the true dispersion. The original motivation for a two-component fit was the long tail in the Δv distribution which could not be satisfactorily accounted for by a one-component model. In § III*a*, we have shown that many, if not all, of the objects in this tail may be due to systematic effects. For these reasons and especially the low velocity dispersion derived for H I clouds (§ III*b*), the use of Δv(H I, H II) for deducing number density and velocity dispersion of H I clouds is questionable.

IV. ENERGETICS AND ORIGIN OF THE HIGH DISPERSION H I

In § III we found that fast H I ($\sigma > 30$ km s^{-1}) indeed does exist. However, our limits on the volume density and the mass fraction in three different regions of the Galaxy are an order of magnitude smaller than the predictions of the RS model. For the purpose of discussion we adopt the following parameters for fast H I: mass fraction $\leq$20%, volume density fraction (at $z = 0$) $\leq$ 4%, and a mean velocity dispersion of 35 km s^{-1}. Using these parameters, we find the surprising result that the kinetic energy in fast H I is greater than the sum of the kinetic energy in the two components of local H I (Table 2). Kinetic energy estimates are very sensitive to the parameters obtained from Gaussian decomposition. In order to avoid this problem and to demonstrate this result in a model-independent way, we display in Figure 9 the quantity $E_k(v) = (3/2)T_B(v)v^2$. Here $T_B(v)$ is the brightness emission for the NGP region and is restricted to $v > 0$ in order not to be confused by the infalling H I. The quantity $E_k(v)$ is simply a measure of the kinetic energy per unit interval in a cylinder of infinite length and unit area (1 cm^{-2}) and is perpendicular to the galactic plane. The surprising and curious result is that $E_k(v)$ appears to be independent of v (Fig. 9). For velocities larger than 80 km s^{-1}, $E_k(v)$ is certainly affected by baseline uncertainties. The quantity $E_k(v)$ is reasonably correct to a factor of 2 for $40 < |v| < 80$ km s^{-1} and is certainly correct for $0 < |v| < 40$ km s^{-1}. Thus, we see that in a

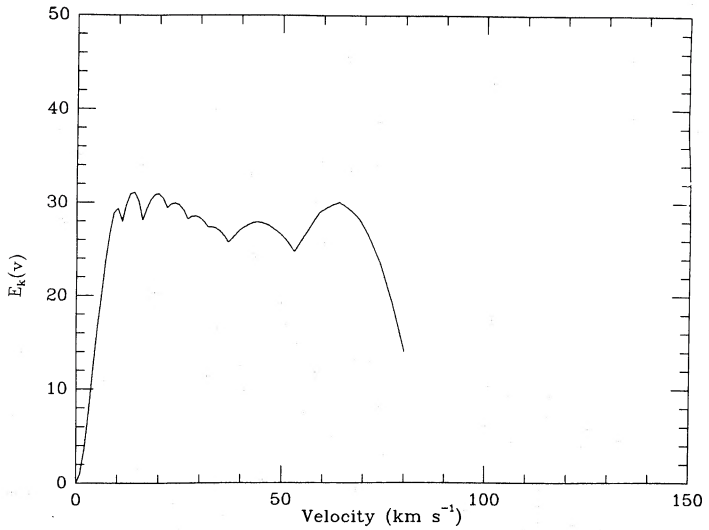

FIG. 9.—Kinetic energy, $E_k(v)$, in H I toward the north galactic pole is plotted at each velocity. In order not to be confused by the infall (§ III*b*), only the positive velocity H I has been used in this plot. The plot has been truncated at $v > 80$ km s^{-1} since baseline uncertainties make the determination of the kinetic energy unreliable beyond this velocity. The units of $E_k(v)$ along the vertical axis are arbitrary.

model-independent way that the kinetic energy in fast H I is larger than in the slow-moving ($\sigma \approx 8$ km s^{-1}) diffuse clouds. This result is of some importance since previously efforts were made to explain only the motion of slow-moving diffuse clouds (e.g., McKee and Ostriker 1977).

Fast H I by the virtue of its higher velocity dispersion surely must have a higher scale height. This expectation is borne out by Figure 10, where we show a low-latitude H I emission profile and superposed on it a plot of $\langle b^2 \rangle^{1/2}$ [defined as $\langle T_B(v) b^2 \rangle / \langle T_B(v) \rangle$, where the angle brackets represent an average over the latitude]. Since the velocity of H I in excess of the subcentral velocity is proportional to the velocity dispersion of H I, we see that fast H I has a scale height much larger than the normal velocity dispersion H I. This is precisely the behavior of the H I in the lower halo that was first noted by Lockman (1984). According to Lockman (1984), in the inner galaxy at least $\sim 10\%$ of the H I lies above $|z|$ of 500 pc and has a larger velocity dispersion than gas at lower z. Thus, fast H I can be identified with the lower halo H I.

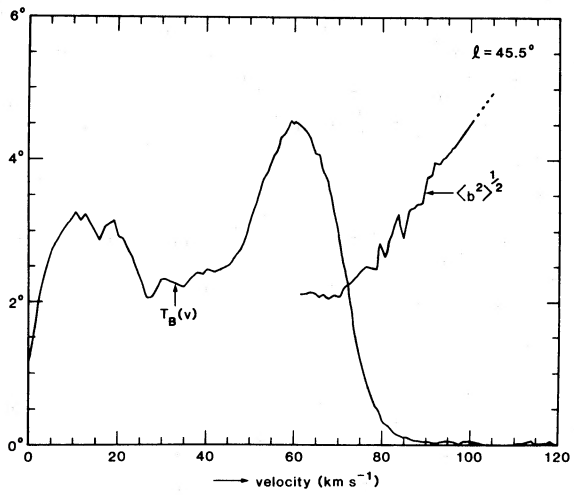

FIG. 10.—Curve marked $T_B(v)$ refers to the H I emission spectrum in the direction $l = 45.5$ and $b = 0°$. Superposed on this spectrum is a plot of the angular scale height, $\langle b^2(v) \rangle^{1/2}$ (§ IV), against the velocity beyond the subcentral velocity. The left-hand vertical axis refers to $\langle b^2 \rangle^{1/2}$.

What is the origin of fast H I and what keeps it stirred up? A simple explanation for fast H I is that it is formed by supernovae. The hot gas in supernova interiors, if unobstructed, will rise to high $|z|$, eventually cool, and condense into H I clouds. These clouds will then fall toward the galactic plane. We now demonstrate that supernovae have more than enough energy to keep this system stirred up.

In order to calculate the energy injection rate into the fast H I system we need to calculate the total kinetic energy in the fast H I system and the mean time between successive inelastic collisions of fast H I clouds. Lockman (1984) has shown that the vertical distribution of H I in the inner Galaxy can be satisfactorily modeled by the sum of three components:

z-component 1: σ_z (Gaussian rms) = 104 pc,
$n_H(0) = 0.16$ atom cm^{-3};
z-component : σ_z (Gaussian rms) = 240 pc,
$n_H(0) = 0.09$ atom cm^{-3};
z-component 3: σ_z (exponential e-folding) = 481 pc,
$n_H(0) = 0.05$ atom cm^{-3}.

The kinetic energy of each of these z-components can be calculated by assuming that the H I layer is in hydrostatic equilibrium with the stellar gravitational field. For simplicity, we also assume that each component of H I is associated with its own cosmic-ray and magnetic field pressure. With these simplifying assumptions, σ_z, the z scale height (in pc) of an H I layer, is linearly related to the σ_v, the velocity dispersion (in km s^{-1}) in the layer (Kellman 1972):

$$\sigma_z = 5 \text{ pc } \alpha \sigma_v (\rho_t / 40 \text{ atoms cm}^{-3})^{-1/2} , \quad (1)$$

where

$$\alpha^2 = (P_{cr}/\rho_{gas} + P_B/\rho_{gas} + \sigma_v^2)/\sigma_v^2 , \quad (2)$$

and P_{cr}, P_B, ρ_{gas} are simply the mean cosmic-ray pressure, the mean magnetic field pressure, and the mean gas density. The variable ρ_t is the total density in atoms cm^{-3} at $z = 0$ pc and has been evaluated at $R = 5$ kpc assuming a disk exponential length scale of 3.5 kpc ($R_0 = 10$ kpc) and a $\rho_t(R_0) = 10$ atom

cm^{-3}. The variable σ_v has been assumed to isotropic. The local value of α^2 is ~ 3 since there appears to be equipartition in the energy densities of cosmic rays, magnetic field, and gas motions (Spitzer 1978).

Equation (1) is really valid only when $\sigma_z \ll \sigma_z^*$, the scale height of stars. Locally, $\sigma_z^* \approx 400$ pc (Spitzer 1978). There are no data for σ_z^* in the inner Galaxy; we have assumed that $\sigma^* > \sigma_z$. Also α is expected to increase with $|z|$ since the magnetic field and the cosmic rays, being more buoyant, float up to larger heights. The linearity of $\langle b^2(v)\rangle^{1/2}$ with increasing velocity deviation from the subcentral point velocity (Fig. 10) suggests that the decrease in stellar density at large z is approximately compensated by an increase in α, σ_v, or both.

Applying equation (1) to each of the three z-components of H I in the inner Galaxy, we obtain the following kinetic energy per cm^{-2} of area perpendicular to the galactic disk: $E_k(1) \approx 1 \times 10^8 \alpha^{-2}$ ergs cm^{-2}, $E_k(2) \approx 8 \times 10^8 \alpha^{-2}$ ergs cm^{-2}, and $E_k(3) \approx 7 \times 10^9 \alpha^{-2}$ ergs cm^{-2}, respectively. The kinetic energy of local H I in similar units [restricted to $|v| < 80$ km s^{-1} and obtained by simply integrating the curve $E_k(v)$ shown in Fig. 9] is 2×10^8 ergs cm^{-2}. Adopting the local value of α, we see that E_k(local) is smaller than the sum of kinetic energy of the three components at $R = 5$ kpc by a factor of 10. A part of this discrepancy is simply due to the fact that the total column density at $R = 5$ kpc, according to the three-component model of Lockman (1984), is $\sim 5 \times 10^{20}$ atoms cm^{-2}, whereas the local column density (Table 2) is $\sim 3 \times 10^{20}$ atoms cm^{-2}. The restricted velocity coverage in estimation of E_k(local) probably does not result in underestimation of E_k(local) by more than a factor of 1.5. If our estimate of $\rho_t(R = 5$ kpc) is correct, then this discrepancy indicates (*a*) $\alpha^2 > 3$ either at high $|z|$ in the inner galaxy or (*b*) the inner galaxy H I is more energetic than local H I, or (*c*) both. Setting aside this interesting result, the important point to note is that the kinetic energy in component 3 is about an order of magnitude larger than that in components 1 and 2 put together—in agreement with the conclusions for local H I.

Supernovae have been invoked to explain the random motions of slow clouds (Spitzer 1978). McKee and Ostriker (1977) show explicitly how the diffuse clouds are kept stirred up by the disruptive cloud-shell collisions in the postcooling interval. A mere 5% of the supernova energy is utilized in stirring normal velocity-dispersion diffuse clouds. Assuming that Lockman's components 1 and 2 represent the normal velocity-dispersion H I clouds, we see that the kinetic energy in his component 3 or our fast H I is about an order of magnitude larger than that of the normal velocity-dispersion clouds. Thus, if the mean time between collisions of fast H I clouds were the same as the normal dispersion clouds, then the energy injection rate will have to be increased by an order of magnitude! This problem is more severe in the RS model where the fast cloud system contains 100 times more energy than the normal dispersion cloud system. RS appreciated this problem and suggested that the velocity field of the fast H I clouds was probably correlated over long enough length scales so that the number of collisions were reduced considerably. We now proceed to estimate the mean time between two inelastic collisions for the fast H I system and show that, indeed, the fast H I clouds take a longer time to collide, but for a somewhat different reason.

From Figure 10 and Lockman's (1984) work, it is clear that fast H I forms an extended layer in $|z|$. These clouds will then fall toward the plane and on encountering the normal velocity-dispersion H I material at low $|z|$ dissipate most of their kinetic energy. Thus, the time scale between successive inelastic collisions is the time to fall from high $|z|$ to the plane. Assuming an average height of this layer to be 500 pc and an average infall velocity of 40 km s^{-1}, this mean time is ~ 25 million years. Thus, the kinetic energy injection rate needed to keep this layer is $E_k(3)/25$ million years $= 10^{-6}$ ergs cm^{-2} s^{-1}. According to Abbot (1982), the *total* energy injected by supernovae in all forms is 10^{-4} ergs cm^{-2} s^{-1}, of which only 5% is needed to keep the normal dispersion cloud system stirred up (McKee and Ostriker 1977). Thus, the fast H I clouds, while containing most of the kinetic energy of the ISM, require nearly an order of magnitude less energy injection rate than their slower moving cousins.

V. SUMMARY

RS, from an analysis of H I absorption profile toward the galactic center, suggested that there exists a new class of lukewarm ($T \leq 100$ K) H I clouds with a velocity dispersion of 35 km s^{-1} ("fast H I clouds"). Studies by A and S of statistics of the difference between the velocity of H II regions and extreme H I absorption velocities lended additional weight to the RS picture. Westerbork synthesis data of the galactic center region of Schwarz, Ekers, and Goss (1982) put an upper limit to the number density of the fast H I clouds. Even with this limit, the total mass of fast H I clouds could be as high as 3 times the total mass in cold H I clouds.

A and S use the statistics of the differences between H II region velocities, and H I absorption velocities can be used to deduce the number density and the velocity dispersion of H I clouds. We agree in principle with this approach. However, we find that these statistics are easily confused by many (known) systematic effects such as the flow of ionized gas out of the H II region, the difference between the velocity of the H II region, and the parental molecular complex, expanding H I shells produced by either a supernova, or stellar winds and/or ionization fronts and pseudo-absorption due to the variations in the H I emission field. After accounting for all these effects, we find that the conclusions of A and S are quite weakened.

We have searched for fast H I clouds in H I emission data. This approach is preferable because H I emission, unlike H I absorption, is not biased toward cooler clouds. We do find evidence for fast H I clouds. However, our firm upper limits are about a factor 10 smaller than that proposed by RS. Roughly our limits are as follows: mass fraction $\leq 20\%$, fractional volume density in the galactic plane $\leq 4\%$, and a mean dispersion of ~ 35 km s^{-1}. The fast H I clouds have a scale height larger than the normal dispersion H I clouds. In fact, fast H I is simply the halo H I that has been recently studied by Lockman (1984).

We find that there appears to be a rough equipartition of kinetic energy of local H I with respect to velocity; i.e., the kinetic energy of local H I is approximately constant from 0 km s^{-1} to ~ 80 km s^{-1}. There is very little gas beyond 100 km s^{-1}, and instrumental difficulties prevent us from measuring the kinetic energy beyond 80 km s^{-1}. This implies that the kinetic energy in the normal dispersion H I ($\sigma \approx 8$ km s^{-1}) is about one-fifth of the kinetic energy of fast H I. We find a similar behavior for H I in the inner Galaxy. Thus, while less than one-fifth of H I is fast H I, the kinetic energy locked up in the fast H I system is 5 times as much as that in the normal dispersion H I. We conjecture that the fast H I is simply but supernova gas that has now cooled. We find that the amount of energy needed to keep the fast H I layer stirred up is only a

fraction of that required to stir the normal dispersion clouds system.

We are indebted to Carl Heiles without whose encouragement this work would not have been completed. We gratefully acknowledge stimulating discussions with K. Anantharamaiah, C. McKee, C. Heiles, V. Radhakrishnan, and A. A. Stark. We wish to thank R. Nityananda for pointing out, in an earlier version, an inconsistency in § IV and clarifying the Parker picture for the z-distribution of magnetic fields and cosmic rays. Lastly, we thank A. A. Stark and C. Heiles for providing the AT&T Bell Laboratories H I survey in a machine-readable form and in advance of the publication of the data.

REFERENCES

Abbot, D. C. 1982, *Ap. J.*, **263**, 723.
Ananthramaiah, K. R., Radhakrishnan, V., and Shaver, P. A. 1984, *Astr. Ap.*, **138**, 131.
Bash, F. N. 1983, in *IAU Symposium 100, Internal Kinematics and Dynamics of Galaxies*, ed. E. Athanassoula (Dordrecht: Reidel), p. 133.
Bash, F. N., and Leisawitz, D. 1984, *Astr. Ap.* in press.
Blitz, L., Fich, M., and Stark, A. A. 1983, *Ap. J. Suppl.*, **49**, 183.
Burton, W. B. 1976, *Ann. Rev. Astr. Ap.*, **14**, 275.
Coulomb, F. R., Popper, W. G., and Heiles, C. 1977, *Astr. Ap. Suppl.*, **29**, 89.
Dickey, J. M., Salpeter, E. E., and Terzian, Y. 1979, *Ap. J.*, **228**, 465.
Fich, M., Treffers, R. R., and Blitz, L. 1982, in *Regions of Recent Star Formation*, ed. R. S. Roger and P. E. Dewdney (Dordrecht: Reidel), pp. 201–208.
Fich, M., and Van Buren, D. 1984, in preparation.
Gillespie, A. R., Huggins, P. J., Sollner, T. C. L. G., and Phillips, T. G. 1977, *Astr. Ap.*, **60**, 221.
Kellman, S. 1972, *Ap. J.*, **175**, 353.
Kulkarni, S. 1983, Ph.D. thesis, University of California, Berkeley.
Lewis, B. M. 1983, NAIC preprint.
Lizst, H. S. 1983, *Ap. J.*, **275**, 163.
Lockman, F. J. 1984, *Ap. J.*, **283**, 90.
McKee, C. F., and Ostriker, J. P. 1977, *Ap. J.*, **218**, 148.
Paresce, F. 1984, Space Telescope Science Institute preprint.
Radhakrishnan, V., and Sarma, N. V. G. 1980, *Astr. Ap.*, **85**, 249.
Radhakrishnan, V., and Srinivasan, G. 1980, *J. Astr. Ap.*, **1**, 47.
Read, P. L. 1980, *M.N.R.A.S.*, **192**, 11.
Roger, R. S., and Pedlar, A. 1981, *Astr. Ap.*, **94**, 238.
Schwarz, U. J., Ekers, R. D., and Goss, W. M. 1982, *Astr. Ap.*, **110**, 100.
Shaver, P. A., Radhakrishnan, V., Ananthramaiah, K. R., Retallack, D. S., Wamsteker, W. W., and Danks, A. C. 1982, *Astr. Ap.*, **106**, 105.
Spitzer, L. 1978, *Physical Processes in the Interstellar Medium* (New York: Wiley-Interscience).
Stark, A. A., Bally, J., Linke, R. A., and Heiles, C. 1984, in preparation.
Van Buren, D. 1983, Ph. D. thesis, University of California, Berkeley.
Weaver, H. 1974, in *Highlights of Astronomy*, Vol. **3**, ed. G. Contopoulos (Dordrecht: Reidel), pp. 423–440.
Weaver, H., and Williams, D. R. W. 1973, *Astr. Ap. Suppl.*, **8**, 1.

MICHEL FICH: Astronomy Department, University of Washington, FM-20, Seattle, WA 98195

SHRINIVAS R. KULKARNI: Radio Astronomy Laboratory, University of California, Berkeley, CA 94720